Soft X-ray Emission Profile and Mode Structure During MHD Events in the TST-2 Spherical Tokamak

H. TOJO, A. EJIRI, Y. TAKASE, Y. TORII, T. OSAKO, M. SASAKI[1)], T. MASUDA, Y. SHIMADA, N. SUMITOMO[1)], J. TSUJIMURA, H. NUGA[1)], S. KAINAGA[1)] and J. SUGIYAMA

Graduate School of Frontier Sciences, The University of Tokyo, Kashiwa 277-8561, Japan
[1)]Graduate School of Science, The University of Tokyo, Tokyo 113-0033, Japan

(Received 4 December 2006 / Accepted 20 April 2007)

Mode structures during MHD events in the TST-2 spherical tokamak are revealed by means of singular value decomposition. Soft X-ray and magnetic coil signals show growths of modes with toroidal mode numbers $n = 1$ and 2. Slow evolution of the soft X-ray profile indicates beginning of localized crash. Occurrence of these events is correlated with the spatial gradient of the soft X-ray profile, suggesting that these events are driven by the pressure gradient. Increases in impurity ion temperatures (CIII and OV) are observed. These are positively correlated with the increment of the plasma current during these events.

Keywords: IRE, spherical tokamak, SVD, soft X-ray, ion temperature, reconnection

DOI: 10.1585/pfr.2.S1065

1. Introduction

In spherical tokamaks (STs), MHD instabilities have different characteristics compared to those in conventional tokamaks. In particular, reconnection events (REs) are known to cause energy and particle losses [1]. Reference [1] showed the process in detail by MHD simulation. First, modes with $m/n = 1/1$ and 2/2 grow predominantly, where m and n are poloidal and toroidal mode numbers, respectively. These modes couple nonlinearly, and deform the plasma. Magnetic field lines which belong to inner closed flux surfaces can reconnect with field lines in the outer open field line region. When such reconnection occurs, the pressure gradient along the reconnected magnetic field line causes plasma energy and particle losses. Such events are studied experimentally on START [2], TST-2 (Tokyo Spherical Tokamak-2) [3] and other ST devices. Objectives of this study are to compare the results of MHD simulation with experimental results in terms of mode behavior (i.e., individual modes and their nonlinear coupling) and to identify the source of instability.

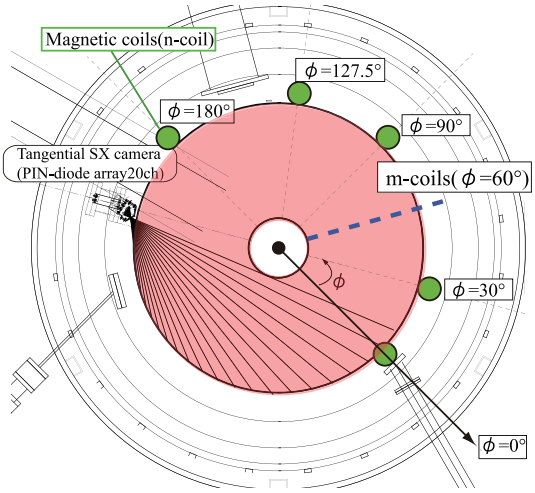

Fig. 1 Top view of TST-2 showing tangential sightlines of the tangential SX camera (black lines) and locations of magnetic coils (n-coils and m-coils).

2. Experimental Setup

2.1 Soft X-ray detectors and filters

MHD mode behavior can be studied by measuring the soft X-ray (SX) emission profile. Pin-hole cameras with a 20-channel PIN-diode array and a 16-channel photo-diode array (AXUV16ELOHYB1: IRD Inc.) were used to measure the SX radiation profile. The sensitive energy ranges for both detectors are from a few eV to 10 keV, and the frequency responses are up to about 100 kHz for the PIN diode and 300 kHz for the AXUV. The sightlines of the PIN-diode array are tangential (toroidal) and cover the entire range of radius occupied by the plasma on the equatorial plane (Fig. 1). The sightlines of the AXUV array is in the poloidal plane and measures the vertical profile of the plasma (Fig. 2).

Either a 7 μm beryllium (Be) filter or a polypropylene (P.P.) filter was placed in front of the pin-hole. Be filter rejects photons with low energies (< 1 keV), whereas P.P. filter has a transparent window around 300 eV, in addition to the high energy range (> 1 keV). A curved filter was used instead of a flat filter to ensure the same filter thickness

author's e-mail: tojo@fusion.k.u-tokyo.ac.jp

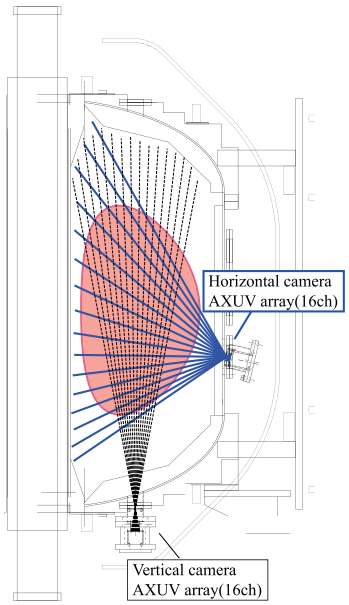

Fig. 2 Sightlines of the horizontal SX camera (16 ch) and the vertical camera (16 ch, under preparation).

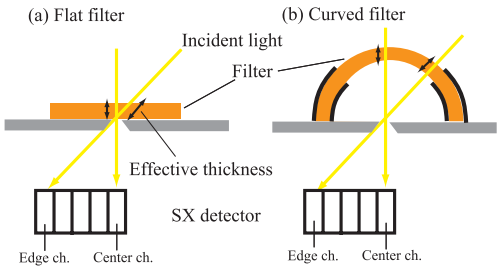

Fig. 3 Schematics of flat (a) and curved (b) filters. The effective thickness is the same for all channels if a curved filter is used.

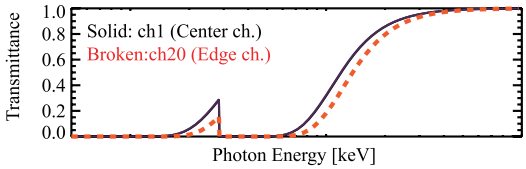

Fig. 4 Transmittance for center and edge channels of the tangential SX camera, showing the effect of oblique incidence for a flat P.P filter.

for each channel in an array (Fig. 3). If a flat filter were used, the effective thickness of the filter (and therefore the transmittance) would vary for different channels (Fig. 4). This would cause a difference by a factor of two in incident power for a typical electron temperature of $T_e = 150$ eV in TST-2, assuming a bremsstrahlung spectrum. Therefore, a curved filter was used to avoid such a systematic distortion.

2.2 Magnetic coils

Magnetic fluctuations are measured by magnetic pick-up coils with a frequency response of up to 50 kHz. These coils are distributed along the toroidal direction (n-coils: 5 ch) and the poloidal direction (m-coils: 7 ch). The toroidal locations of the n-coils are shown in Fig. 1. The m-coils are located at poloidal angles of $\theta = 0°$, 40°, 120°, 150°, 190°, 240°, and 320° on the same poloidal plane at $\phi = 60°$.

2.3 Mode analysis by singular value decomposition

Singular value decomposition (SVD) [4] has been used to analyze mode structures in many fusion experiments [5]. Consider a matrix $A(M \times N)$, which can be expressed as

$$A = U\Sigma V^T, \tag{1}$$

where U $(M \times M)$ and V $(N \times N)$ are orthogonal matrices and Σ $(M \times N)$ is a diagonal matrix.

By using column vectors $\vec{u}_i$ and $\vec{v}_i$, this can be expressed as

$$A = [\vec{u}_1, \vec{u}_2 \cdots, \vec{u}_M] \begin{bmatrix} \sigma_1 & & & & \\ & \sigma_2 & & 0 & \\ & & \ddots & & 0 \\ & 0 & & \ddots & \\ & & & & \sigma_M \end{bmatrix} \begin{bmatrix} \vec{v}_1^T \\ \vec{v}_2^T \\ \vdots \\ \vdots \\ \vec{v}_N^T \end{bmatrix} \tag{2}$$

This equation indicates that A can be expressed as the sum of $\sigma_i u_i v_i^T$, where σ_i, u_i, and v_i are called the singular value (power of the ith mode), chrono, and topo, respectively. In order to apply this method to experimental data, we define the matrix A as

$$A = \begin{bmatrix} a_1(0) & a_2(0) & \cdots & a_N(0) \\ a_1(\Delta t) & a_2(\Delta t) & \cdots & a_N(\Delta t) \\ \vdots & \vdots & \ddots & \vdots \\ a_1((M-1)\Delta t) & a_2((M-1)\Delta t) & \cdots & a_N((M-1)\Delta t) \end{bmatrix}. \tag{3}$$

The numbers of columns and rows are equal to the numbers of channels (N) and time samples (M), respectively. Chrono and topo show common waveforms for all channels (temporal eigenmodes) and distribution of chrono (spatial eigenmodes), respectively. Time evolutions of each decomposed mode (i.e., chrono) and its spatial distribution (i.e., topo) can be extracted in this way. As mentioned above, the mode structure is useful for comparing experimental data with theory. In most SVD analyses on other fusion devices, only SX signals are used. In our case, magnetic signals from pick-up coils, distributed along the toroidal and poloidal directions, are used in addition to SX signals.

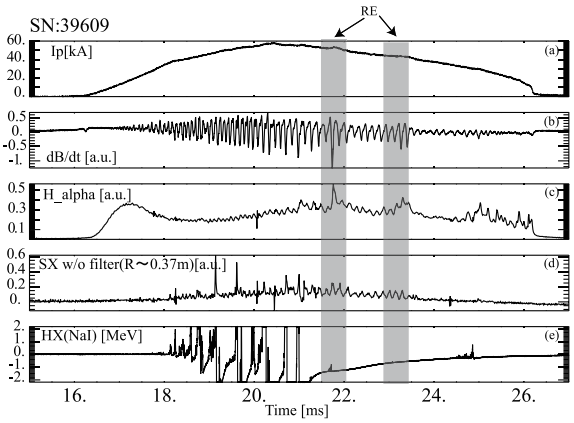

Fig. 5 Typical discharge waveforms with REs (SN39609). (a) plasma current, (b) signal from a magnetic pick-up coil, (c) H_α emission, (d) SX signal from PIN-diode ($R \sim 0.37$ m), (e) hard X-ray signal from NaI (Tl) scintillator.

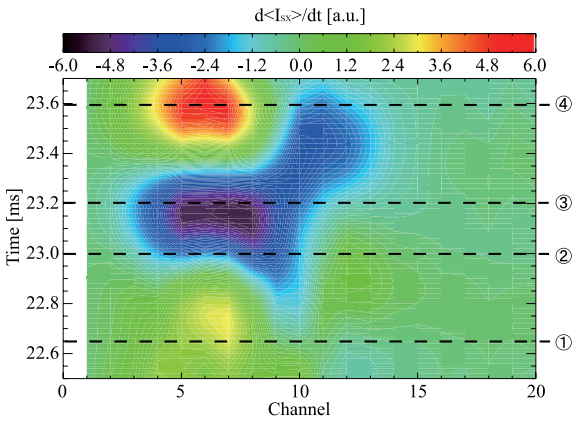

Fig. 6 Profile of $d\langle I_{SX}\rangle/dt$ during an RE (SN39609). The channel number represent the radial direction (ch. 1 corresponds to the innermost sightline, tangentially).

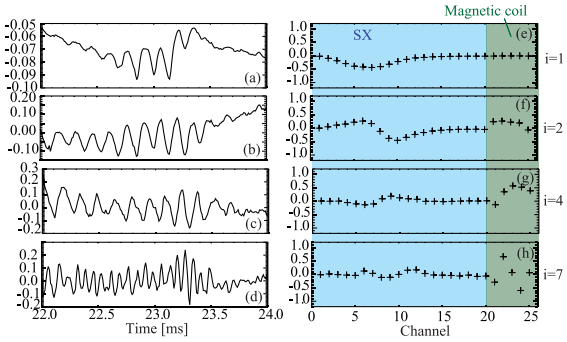

Fig. 7 Chrono (a)-(d) and topo (e)-(h) of tangential SX camera and *n*-coils for modes $i = 1$, 2, 4, and 7 (SN39609).

3. Experimental Results and Discussion

3.1 Typical discharge

Figure 5 shows a typical discharge with REs. RE occurred at least twice in this discharge. The plasma current (I_p) increases slightly in response to a flattening of the current density profile (reduction of the internal inductance). Prior to each RE, a growth of a mode at a frequency of around 10 kHz was observed in SX emission (especially low energy emission measured by the camera without a Be filter) and in magnetic signals from pick-up coils. In many cases, the SX intensities increase, and the mode amplitude grows with a time scale constant of about 0.4 ms. On the other hand, intensities of magnetic oscillations generally shows growths on a shorter time scale (~ 0.1 ms). At the end of mode growth, energy loss from the central region towards the plasma periphery begins. Following this collapse, the SX intensities in the outer region increase, and the H_α emission increases. This can be explained by increased interaction of the lost plasma with the limiter or the vacuum vessel wall. The crash time determined by the duration of the decrease of SX intensity near the plasma center is typically 0.05-0.1 ms. RE in this study is defined as those accompanying a growth of oscillations on SX intensities and magnetic signals, and a crash of SX intensity. In some cases a crash is not observed on SX intensity measured with filters.

3.2 Slow time evolution

In order to analyze the slow behavior of energy transport, the profile of $d\langle I_{SX}\rangle/dt$ is plotted in Fig. 6, where $\langle I_{SX}\rangle$ is the time-averaged intensity of SX obtained by low pass filtering (< 3 kHz). This figure clarifies the energy loss process during an RE. At 22.65 ms (① in Fig. 6) the intensity starts to decrease near the center of the plasma, around ch10 ($\rho \sim 0.2$), indicating that a reconnection started around ①. From ② to ③ the decay region expands toward the center and then toward the outboard side of the plasma. At ④ the SX intensity at the center has recovered.

3.3 SVD analysis during the growth phase

Magnetic signals reflect mainly the outer mode behavior of the plasma, while SX signals reflect the core behavior. SVD analysis including magnetic signals is useful to obtain correlation between outer and core phenomena. SVD was performed on SN39609 using data from the tangential SX camera (without filter) and *n*-coils (5 channels). Chrono and topo are shown in Fig. 7. The dominant mode ($i = 1$) grew until $t \sim 23.3$ ms (Fig. 7 (a)). The poloidal mode number is even for this mode, as shown in Fig. 7 (e). The secondary mode ($i = 2$) grows with odd poloidal mode number and shows a small correlation with the toroidal mode. Modes $i = 4$ and 7 correspond to $n = 1$ and 2, respectively, because magnetic coils in chrono show half a period for $i = 4$ and one period for $i = 7$. Moreover, the $i = 7$ mode has twice higher frequency compared to the $i = 4$ mode. From these results, during the growth phase (~ 23.3 ms), the existence of $n = 1$ and 2 modes and small

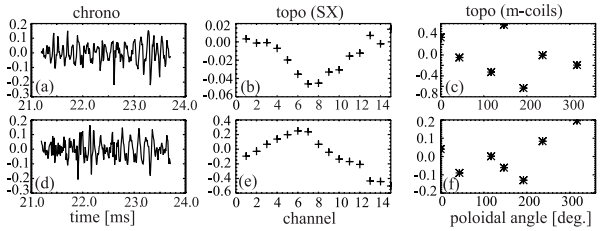

Fig. 8 Chrono ((a), (d)), topo of the horizontal SX camera ((b), (e)) and, topo of the m-coils ((c), (f)). Modes $i = 1$ and 8 correspond to (a)-(c) and (d)-(f), respectively (SN46513).

effects on the SX profile are clarified.

SVD was applied to horizontal SX camera and *m*-coil data. In this experiment, the P.P. curved filter was used for the SX camera and only fluctuating components (5-40 kHz) were analyzed. The dominant mode ($i = 1$) shows a growth of even mode until just before the crash, and the magnetic topo shows some correlation to this fluctuation (Fig. 8 (a), (c)). Note that the intensity of fluctuations measured by m-coils depends strongly on plasma position. Therefore, there are many cases for which we cannot determine the poloidal mode number. For $i = 8$, SX topo shows an odd-mode (Fig. 8 (b)). It is believed that channels 9-11 correspond to the plasma center in this discharge. In some cases, during the growth phase an even-mode is dominant and odd-mode is weak. However, sometimes SX fluctuations do not show growth but magnetic fluctuations show growth with a short time scale.

3.4 Correlation between SX gradient and ΔI_p

Identification of the condition or energy source for this instability is very important for its prevention. We define the spatial gradient of SX intensity, $\mathrm{d}I_{SX}/\mathrm{d}r$, where I_{SX} is the SX intensity (without filter) and r is the tangency radius of the sightline. The gradient is taken from a linear fit to the SX intensity profile on the outboard side of the torus. Figure 9 indicates that a steep profile is necessary to cause an RE. The threshold is around $\mathrm{d}I_{SX}/\mathrm{d}r = 0.02$. This result suggests that the instability is pressure driven, because SX intensity depends strongly on the plasma pressure. A positive correlation between $\mathrm{d}I_{SX}/\mathrm{d}r$ and $\Delta I_p/I_p$, which is a measure of the strength of RE, was also confirmed. Here ΔI_p is the increment of I_p during an RE. It indicates that a steeper SX profile induces a larger RE.

3.5 Ion temperature increase

Magnetic reconnection releases magnetic energy. Increases of ion-temperature (T_i) have been observed in MAST [6] and TST-2 [7]. Sudden increases of ion temperature suggest the occurrence of magnetic reconnection. Figure 10 shows the correlation between $\Delta T_i/T_i$ and $\Delta I_p/I_p$, where $\Delta T_i/T_i$ is the relative increment of ion temperature due to RE. The ion temperature was measured by Doppler broadening of CIII and OV lines. Typically T_i (CIII) ~ 20 eV and T_i (OV) ~ 40 eV before RE. All data points in the plot show growth of magnetic and/or SX fluctuations. T_i measured by CIII and OV are correlated positively with $\Delta I_p/I_p$. Especially, the highest increment of $\Delta T_i/T_i \sim 2.4$ was measured by OV. The scale of RE (represented by $\Delta I_p/I_p$) is positively correlated with the increase of T_i, indicating that large scale REs result in stronger ion heating.

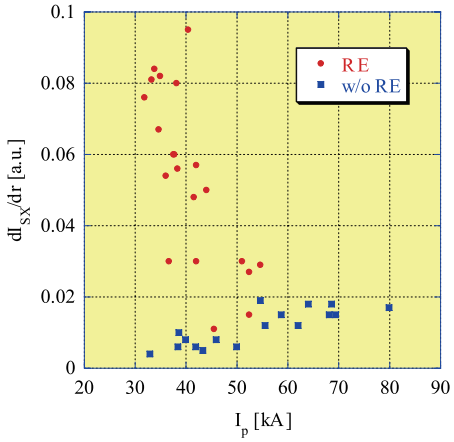

Fig. 9 $\mathrm{d}I_{SX}/\mathrm{d}r$ for discharges with RE (red circles) and without RE (blue squares) for various values of I_p.

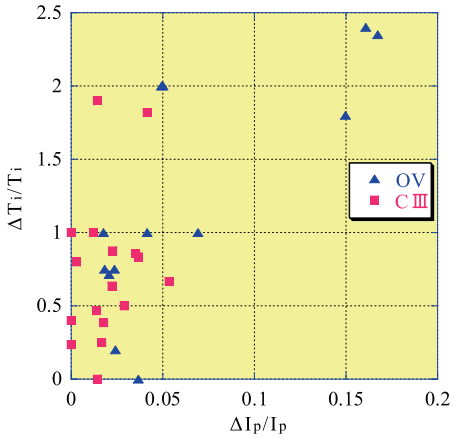

Fig. 10 Correlation between $\Delta T_i/T_i$ and $\Delta I_p/I_p$. CIII and OV are presented by red squares and blue triangles.

4. Conclusion and Summary

Simultaneous SVD analysis of SX intensities and magnetic signals is effective for studying the mode structure. From the temporal eigenmodes of SX intensity, the co-existence of even and odd modes was observed during the growth phase, and toroidal mode numbers of $n = 1$ and 2 were confirmed. The existence of these modes is consistent with the results of MHD simulation. From the spatial gradient of the SX profile, the pressure gradient was sug-

gested as a candidate to drive this instability. The threshold for instability was $dI_{SX}/dr \sim 0.02$. The measured ion heating was also consistent with other experiments, and a positive correlation with $\Delta I_p/I_p$ showed evidence of conversion of magnetic energy to ion thermal energy.

Acknowledgments

This work was supported by JSPS (Japan Society for the Promotion of Science) Grant-in-Aid for Scientific Research No. 16106013.

[1] N. Mizuguchi *et al.*, Phys. Plasmas **7**, 940 (2000).
[2] A. Sykes *et al.*, Plasma Phys. Control. Fusion **39**, B247 (1997)
[3] Y. Takase *et al.*, Nucl. Fusion **41**, 1543 (2001).
[4] C. Nardone, Plasma Phys. Control. Fusion **34**, 1447 (1992)
[5] S. Yoshimura *et al.*, Nucl. Fusion **9**, 3378 (2002).
[6] P. Helander *et al.*, Phys. Rev. Lett. **89**, 235002 (2002).
[7] A. Ejiri *et al.*, Nucl. Fusion **43**, 547 (2003).